Persistent spectral hole burning spectroscopy of the $T_{1u} \leftarrow A_{1g}$ (690 nm) line in the $CaF_2:Sm^{2+}$ system

W. Beck, D. Ricard, and C. Flytzanis
Laboratoire d'Optique Quantique du CNRS, Ecole Polytechnique, 91128 Palaiseau Cedex, France
(Received 17 February 1998; revised manuscript received 28 May 1998)

We use persistent spectral hole burning to simultaneously measure the homogeneous linewidth and the frequency shift of the lowest one-photon allowed transition of the $CaF_2:Sm^{2+}$system. A nonmonotonous temperature dependence is observed for the frequency shift. Our measurements for both width and shift indicate that the dominant dephasing process is a direct one-phonon absorption process, the (acoustic) phonon frequency being ~ 45 cm^{-1}. This means that the Sm^{2+}ion possesses a level ~ 45 cm^{-1} above the T_{1u} level. Our discussion suggests that this is the T_{2u} level. The inhomogeneous distribution is Lorentzian and its width and position depend on the Sm^{3+} concentration (the Sm^{3+}-F^- complexes acting as point defects) exactly as predicted by theory. [S0163-1829(98)00842-X]

I. INTRODUCTION

Coupling between a system and its environment leads to dephasing processes through which the lines of the system acquire a homogeneous width and their frequency is slightly shifted. Knowledge and understanding of the dephasing processes is important from both the basic physics and the applications viewpoints. Persistent spectral hole burning (PSHB), which has been observed in a large number of materials,[1] is the only spectroscopic technique which allows a simultaneous measurement of the homogeneous width and frequency shift for inhomogeneously broadened transitions. In the case of rare-earth ions doped in crystalline matrices, electron-phonon coupling is usually the main cause for broadening. Homogeneous broadening and frequency shifts induced by electron-phonon coupling have been extensively studied. The theory was developed long ago, especially for the case of acoustic phonons in the Debye approximation.[2] We have recently[3] reconsidered the problem and extended the theory to more general situations. We have also applied our results to the case of the $^7F_1 \leftarrow ^7F_0$ transition of the $CaF_2:Sm^{2+}$ system.[3] $^7F_0$ is the ground state of the Sm^{2+} ion and $^7F_1$ is its first excited state. We have shown that, in this case, the dominant broadening mechanism is pure dephasing due to Raman scattering of TO phonons.

Here, we consider the transition from the ground $4f^6$, $^7F_0$, A_{1g}, state to the $4f^5 5d$, $^7K_4$, T_{1u} excited state of the Sm^{2+} ion in the same CaF_2 matrix. It is one-photon allowed and gives rise, at low enough temperature, to a narrow line at about 690 nm. In this paper, we will call this line the 690-nm line. This transition has already been studied using a polarization sensitive technique.[4] In interpreting their data, the authors of Ref. 4 assumed that the width they were measuring was the homogeneous width of the line and they concluded that a Raman process involving acoustic phonons was responsible for the line broadening. In the present work, we use PSHB to elucidate the dephasing mechanisms for this 690 nm line. PSHB in this line was observed as early as 1984.[5] We will see that the general formalism of Ref. 3 also allows one to analyze our present results and that homogeneous broadening of the 690 nm line is mainly due to a direct one-phonon absorption process. The parameters taken from the theoretical fit to the temperature dependence of the width allow us to calculate the exact temperature dependence of the frequency shift in perfect agreement with the experiment. A nonmonotonous temperature-dependent frequency shift is thus observed and explained.

This paper is organized as follows. We first give experimental details on the samples, apparatus and techniques in Sec. II. Section III is devoted to theoretical considerations: The way the homogeneous width is obtained from the hole width is discussed and the relevant results of electron-phonon broadening theory are briefly recalled. In Sec. IV, we finally give the experimental results and the discussion leading to the aforementioned conclusions. Other observations such as the concentration-dependent inhomogeneous (and homogeneous) width are also discussed.

II. EXPERIMENTAL DETAILS

We have studied four different samples of Sm-doped CaF_2. We will denote them samples *A*, *B*, *C*, and *D*. Divalent samarium ions can be obtained by mainly two ways. Samples *A* and *B* have been obtained by growing the Sm-doped crystals in an inert or slightly reducing atmosphere. In this case, a small part of the samarium substitutes as Sm^{2+} ions for Ca^{2+} ions. This readily leads to green-colored samples. Samples *C* and *D* were not grown in a reducing atmosphere. They only contained Sm^{3+} ions and were colorless. They were subsequently irradiated with a 10 Mrad dose of γ rays from a ^{60}Co source. In this way, part of the Sm^{3+} ions are reduced to Sm^{2+} and defects are created. It has recently been shown[6] that these defects are self-trapped hole pairs. After γ irradiation, these samples also acquire the green color characteristic of Sm^{2+}. In all four samples, only part of the samarium is present as Sm^{2+}, most of it being Sm^{3+}. The Sm^{2+} ions occupy sites of cubic (O_h) symmetry. The Sm^{2+} (Sm^{3+}) concentration as determined from the absorption coefficient at the wavelength 617 nm (1200 nm) (Ref. 7) is given for samples *A*–*D* in Table I.

It is known[5] that under red or green light irradiation,

TABLE I. $Sm^{3+}$and Sm^{2+} concentrations in mol% for our four samples.

Sample	*A*	*B*	*C*	*D*
Sm^{3+}	0.44	0.05	0.73	0.3
Sm^{2+}	7.4×10^{-3}	2.5×10^{-3}	1.9×10^{-3}	1.55×10^{-3}

Sm^{2+} can be photoionized into Sm^{3+}. In this paper, we will concentrate on laser irradiation at ~690 nm corresponding to our 690 nm $T_{1u}\leftarrow A_{1g}$ transition. For sample *A*, the ejected electron is trapped at Sm^{3+} dimers or trimers.[8] For samples *C* and *D*, it has recently been shown[6] that the ejected electron is trapped at self-trapped hole pairs turning them into self-trapped holes which are stable at low temperature (below 135 K). Because of site distribution, the 690 nm line is inhomogeneously broadened below typically 30 K. Using monochromatic light, photoionization is then site selective and leads to PSHB.

For samples *A*, *C*, and *D*, hole burning was obtained using a tunable nanosecond dye laser pumped by a frequency doubled *Q*-switched Nd:YAG laser. This dye laser has a 5 ns pulse duration, a wavelength of ~690 nm, a 50 pulses per second repetition rate and a spectral width of 0.05 cm^{-1}. With this laser alone, we could not burn holes in sample *B*. We could only burn holes in this case by simultaneous irradiation with two dye lasers, one at ~690 nm, the other one at 558 nm, in other words resorting to photon-gated hole burning.[9] The Sm concentration is indeed smaller in sample *B* leading to a larger distance between the Sm^{2+} ions and the electron traps which may possibly be Sm^{3+}-F^-centers. The green photons are then necessary to promote the electron from the T_{1u} or A_{1u} states (see Fig. 1) to the conduction band of the matrix.

Our aim is here to measure the hole shape, its width and position and then deduce from this information about the homogeneous broadening of the 690 nm line. In order to understand the broadening mechanisms, we performed temperature-dependent measurements. To this end, the sample was placed in a cryorefrigerator and the temperature could be lowered down to 8 K. The temperature stability was better than 0.05 K.

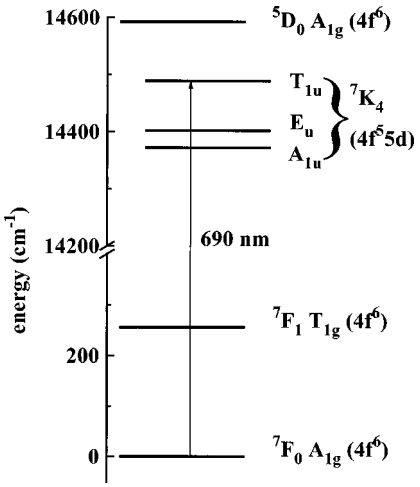

FIG. 1. The energy levels of Sm^{2+} ions (site of cubic symmetry in CaF_2) that are of relevance in the present work. The 690 nm transition is indicated by the vertical arrow.

We used two different techniques to measure the hole profile. In the simpler one, we measure the transmission spectrum before burning the hole and after having burned it. We then take the logarithm of the ratio of the two spectra. In this case, in order to have a reasonable signal-to-noise ratio, the maximum change in absorption coefficient must be a few percent of the initial value. The absorbance of the sample must also be small enough if we want spatially homogeneous excitation. In a more sensitive technique, we burn the hole with two interfering beams 1 and 2. In the reading step, we block beam 2 and detect the light diffracted from beam 1 in the direction of former beam 2. Using this holographic technique,[10,11] the measurement of the diffracted beam intensity directly yields the hole profile when restricting oneself to shallow holes. The holographic technique is much more sensitive than the transmission measurement. Unfortunately, it cannot be used for scattering samples since then the scattered light interferes with the diffracted one. But when both techniques could be used, we checked that they gave identical results. For both techniques, the reading beam intensity was approximately 100 times smaller than the writing intensity.

We also took simple linear-absorption spectra. They are obtained from transmission spectra. In all the measurements discussed here, the reading dye laser is scanned over a narrow range, typically a few cm^{-1}, and for each wavelength, the transmission is averaged over 50 laser shots.

III. THEORETICAL CONSIDERATIONS

A. Measuring the homogeneous linewidth

In spectral hole burning spectroscopy, we measure the hole width. With PSHB, there is no coherent contribution since the writing and reading steps are temporally separated. We must then obtain the homogeneous linewidth from the hole width. For a given line, the linear-absorption coefficient at frequency ω is given by

$$\alpha(\omega)=\int \alpha_{\mathrm{hom}}(\omega-\omega_0)w(\omega_0)d\omega_0, \tag{1}$$

where $\alpha_{\mathrm{hom}}(\omega-\omega_0)$ is the homogeneous spectrum and $w(\omega_0)$ the inhomogeneous distribution for the central frequency. As we will see, the global profile of the 690 nm line is Lorentzian which implies that $w(\omega_0)$ is also Lorentzian. This is often observed for rare-earth ions doped in crystals and has been explained theoretically.[12] In the simplest hole burning case, the number of sites whose central frequency is ω_0 and which are ionized is proportional to $w(\omega_0)\alpha_{\mathrm{hom}}(\omega_p-\omega_0)$ where ω_p is the pump frequency. The hole profile is then given by

$$\delta\alpha(\omega_t;\omega_p)\propto \int w(\omega_0)\alpha_{\mathrm{hom}}(\omega_p-\omega_0)\alpha_{\mathrm{hom}}(\omega_t-\omega_0)d\omega_0. \tag{2}$$

$\delta\alpha(\omega_t;\omega_p)$is the change in absorption coefficient at the test frequency ω_t induced by the pump of frequency ω_p. When the homogeneous width is much smaller than the inhomogeneous one, the factor $w(\omega_0)$ may be taken outside the integral and then

$$\delta\alpha(\omega_t;\omega_p)\propto\int \alpha_{hom}(\omega_p-\omega_0)\times\alpha_{\rm hom}[\omega_t-\omega_p-(\omega_0-\omega_p)]d\omega_0, \quad (3)$$

which is the convolution of the homogeneous profile with itself. The half-width of the hole is then the sum of the homogeneous half-widths Γ_p and Γ_t for the pumping (or writing) and testing (or reading) steps. In this paper, following the notations of Ref. 3, Γ denotes the half-width or dephasing rate in rad/s.

The first complication may arise from saturation. In the steady-state regime, several situations have been considered in Ref. 13. In our case, electrons quickly relax from level T_{1u} to level A_{1u} (see Fig. 1): the population of level T_{1u} is negligibly small. Furthermore, on the timescale of a laser pulse, 5 ns, repopulation of the ground state may be neglected: we are in the transient regime. In such a situation, broadening of the hole due to saturation has already been considered in the case of a one-photon photoionization process.[14] The number of ionized ions at frequency ω_0 after an irradiation time τ is

$$w(\omega_0)(1-e^{-\gamma'\alpha_{\rm hom}(\omega_p-\omega_0)\tau})$$

with $\gamma'=\eta\overline{I}/N\hbar\omega_p$, η being the ionization yield, $\overline{I}$ is the mean laser intensity, and N is the number density of Sm^{2+} ions. Equation (2) must then be replaced by the more general formula:

$$\delta\alpha(\omega_t;\omega_p)=\int w(\omega_0)(1-e^{-\gamma'\alpha_{\rm hom}(\omega_p-\omega_0)\tau})\times\alpha_{\rm hom}(\omega_t-\omega_0)d\omega. \quad (4)$$

When the exponent $\gamma'\alpha_{\rm hom}(\omega_p-\omega_0)\tau$ is small, we recover Eq. (2). When it is large, the central factor in the integral in Eq. (4) goes to 1 and the ''hole'' profile is simply the linear absorption profile of Eq. (1). Equation (4) may be integrated numerically. Saturation broadening may also take place within a single laser pulse as observed under similar circumstances.[15] The relevant quantity is the intensity $\times$duration product, i.e., the irradiation dose and, at low saturation level, the width increases linearly with both I and τ.

When we have a two-photon process, then in the general case γ' is proportional to $\overline{I}^2$ and the relevant quantity is the intensity squared$\times$duration product. If, however, one of the two steps is a rate-limiting step, then the one-photon case results apply. As implied by Eq. (4), we finally observe that saturation may be important in the writing phase. It does not perturb the reading phase since the reading intensity is much smaller.

Even in the absence of saturation, the hole half-width is not always equal to $\Gamma_p+\Gamma_t$ as implied by Eq. (3). As is well known,[16] this is true only when the inhomogeneous width is much larger than the homogeneous one. In the opposite limiting case, the line is homogeneously broadened and the ''hole'' half-width is simply Γ_t. To discuss this problem, we will consider two different situations and anticipate on the experimental results to be presented in Sec. IV.

We first consider the case where writing and reading are performed at the same temperature T. We will see in Sec. IV that, for sample B, the inhomogeneous width $\Gamma_{\rm inhom}$ of this line is 1.57 cm^{-1} and that the largest homogeneous half-width $\Gamma(T)$ we will encounter is about 1.2 cm^{-1}. We numerically calculated the integral in Eq. (2), the first factor being a Lorentzian of full width $\Gamma_{\rm inhom}$ and the other two factors being Lorentzians of half-width $\Gamma(T)$. We varied $\Gamma(T)$ from 0 to 1.2 cm^{-1} and calculated the ratio of the hole half-width to $\Gamma(T)$. The results are plotted in Fig. 2(a) and show a ratio decreasing from 2 to 1. Thus, writing and reading at the same temperature would not be a simple way of measuring $\Gamma(T)$.

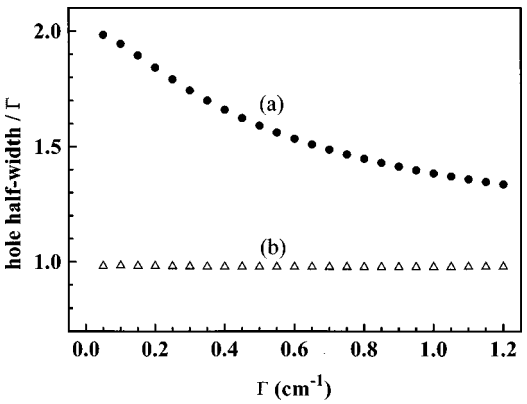

FIG. 2. The calculated value of the ratio of the hole half-width to the dephasing rate Γ: (a) when writing and reading at the same temperature, (b) when writing at low temperature. In case *b*, the homogeneous half-width during the writing phase is $\Gamma(T=0)=0.07$ cm^{-1} and $\Gamma(T=0)$ is subtracted from the hole half-width before dividing by Γ. The inhomogeneous width is 1.57 cm^{-1}.

We then consider the case where writing is performed at very low temperature and reading at temperature T. We will see in Sec. IV that, for sample B again, $\Gamma(T=0\ \text{K})$ is about 0.07 cm^{-1}. Again we numerically calculated the integral in Eq. (2), the second factor being now a Lorentzian of half-width $\Gamma(0)$ and the third factor a Lorentzian of half-width $\Gamma(T)$. We varied again $\Gamma(T)$ from 0 to 1.2 cm^{-1} and calculated the ratio of the hole half-width minus $\Gamma(0)$ to $\Gamma(T)$. The results are plotted in Fig. 2(b) and show a ratio that remains constant and equal to 1 within 2%. Following this procedure, we can then reliably measure $\Gamma(T)$. This is due to the smallness of $\Gamma(0)$ compared to $\Gamma_{\rm inhom}$: only a very narrow class of sites has been excited. This procedure has a further advantage: burning the hole at very low temperature, then reading it at various different temperatures, we study the same class of sites.

B. Electron-phonon interaction

We now give the results for the broadening and frequency shift theory that we will need to interpret the experimental results. Coupling between the system, a Sm^{2+} ion here, and its environment or bath leads to a finite lifetime for the eigenstates of the system's Hamiltonian H_S, to dephasing of the off-diagonal matrix elements of the system's density matrix σ and to a frequency shift for the transitions. The environment consists of the phonons of the CaF_2 matrix. We will often refer to the formalism given in Ref. 3 and use the same notations. The interaction Hamiltonian is written as V_1+V_2 with

$$V_1 = C\sum_k \left(\frac{\hbar\omega_k}{2Mv^2}\right)^{1/2}(a_k - a_k^+) \tag{5}$$

and

$$V_2 = D\sum_k \sum_{k'} \left(\frac{\hbar\omega_k}{2Mv^2}\right)^{1/2}\left(\frac{\hbar\omega_{k'}}{2Mv^2}\right)^{1/2}(a_k - a_k^+)(a_{k'} - a_{k'}^+). \tag{6}$$

C and D are operators acting on the system, k (or k') labels the phonon mode, ω_k is the phonon angular frequency, M is the mass of the crystal, v is the average sound velocity, and a_k and a_k^+ are the phonon annihilation and creation operators.

The transition probability for the system to go per unit time from any given eigenstate, say a, to a different eigenstate, say c, of H_S by one-phonon absorption ($E_c > E_a$) is

$$W_{a\to c}^d = \frac{2\pi}{\hbar^2}|C_{ca}|^2 \frac{\hbar\omega_{ca}}{2Mv^2} p_0(\omega_{ca})\rho(\omega_{ca}), \tag{7}$$

where the superscript d stands for direct: One-phonon processes are also called direct processes. $C_{ca} = \langle c|C|a\rangle$, $\omega_{ca} = (E_c - E_a)/\hbar$, $p_0(\omega) = [e^{\hbar\omega/k_BT} - 1]^{-1}$ is the mean phonon occupation number, ρ is the phonon density of modes, and k_B is Boltzmann's constant. For one-phonon emission ($E_c < E_a$), the rate is simply obtained by replacing ω_{ca} with ω_{ac} and p_0 with $p_0 + 1$. Two-phonon processes such as (phonon) Raman transitions involve matrix elements of D to the second power or of C to the fourth power. When direct transitions are present, two-phonon ones may usually be neglected. Summing the transition rates $W_{a\to c}$ over all states c different from state a, one gets the inverse lifetime of state a.

If we concentrate on a given a-b transition of the system, the decay rate Γ_{ab} (also denoted $1/T_{2ab}$) of the coherence σ_{ab} is half the homogeneous width of this transition. It is made of two contributions $\Gamma_{ab} = \Gamma_{ab}^{\text{non ad}} + \Gamma_{ab}^{\text{ad}}$ (this is equivalent to writing $1/T_2 = 1/(2T_1) + 1/T_2^*$) with

$$\Gamma_{ab}^{\text{non ad}} = \frac{1}{2}\left(\sum_{c\neq b} W_{b\to c} + \sum_{c\neq a} W_{a\to c}\right). \tag{8}$$

This first contribution is known as lifetime broadening. The second contribution is known as pure dephasing or adiabatic broadening. It is totally due to Raman processes and is given by Eq. (19) in Ref. 3.

The frequency shift Δ_{ab} of the a-b transition is $(\Delta E_a - \Delta E_b)/\hbar$, ΔE_a being mainly the sum of two contributions. The first contribution is obtained in second order using V_1 as the perturbation:

$$\Delta E_a^{(2)} = \sum_l |C_{al}|^2 \left(\frac{\hbar}{2Mv^2}\right) P\int \rho(\omega)\omega\left(\frac{p_0(\omega)}{E_a - E_l + \hbar\omega} + \frac{p_0(\omega)+1}{E_a - E_l - \hbar\omega}\right)d\omega, \tag{9}$$

where l is any eigenstate of H_S and P denotes the Cauchy principal value. The second contribution is obtained in first order using V_2 as the perturbation and is given by Eq. (22) in Ref. 3.

Several processes may contribute to the homogeneous width $2\Gamma_{ab}$ of the a-b transition and to its frequency shift Δ_{ab}. Anticipating Sec. IV, we may have a direct one-phonon absorption process from state a to a certain state c. It contributes to the width via lifetime broadening. According to Eq. (8), this width is $2\Gamma_{ab}^d = W_{a\to c}^d$, the latter being given by Eq. (7). Again, the superscript d stands for direct. At this stage, a may be either the lower, A_{1g} in our case, or the upper, T_{1u}, level of the transition. In the case of acoustic phonons, using the Debye approximation for which $\rho(\omega) = 3L^3\omega^2/(2\pi^2 v^3)$ where L^3 is the volume of the crystal, we get

$$2\Gamma_{ab}^d = \frac{2\pi}{\hbar^2}|C_{ca}|^2 \frac{3\hbar}{4\pi^2\rho v^5}\omega_{ca}^3 p_0(\omega_{ca}), \tag{10}$$

where ρ is the density of the crystal. This direct process also contributes to the frequency shift, see Eq. (9), by the amount

$$\Delta_{ab}^d = \frac{1}{\hbar^2}|C_{ca}|^2 \frac{\hbar}{2Mv^2} P\int \rho(\omega)\omega\left(\frac{p_0(\omega)}{\omega - \omega_{ca}} - \frac{p_0(\omega)+1}{\omega + \omega_{ca}}\right)d\omega, \tag{11}$$

which, using the Debye approximation, setting $x = \hbar\omega/k_BT$ and $T_{ca} = \hbar\omega_{ca}/k_B$, leads to

$$\Delta_{ab}^d = \frac{1}{\hbar^2}|C_{ca}|^2 \frac{3\hbar}{4\pi^2\rho v^5}\left(\frac{k_BT}{\hbar}\right)^3 \times P\left(\int_0^{\theta_D/T} \frac{x^3}{x - T_{ca}/T}\frac{1}{e^x - 1}dx - \int_0^{\theta_D/T} \frac{x^3}{x + T_{ca}/T}\frac{e^x}{e^x - 1}dx\right), \tag{12}$$

where θ_D is the Debye temperature. If we are interested in the temperature dependence, Eqs. (10) and (12) may be written

$$2\Gamma_{ab}^d = \overline{\beta} p_0(\omega_{ca}), \tag{13a}$$

$$\Delta_{ab}^d = \beta\left(\frac{T}{T_{ca}}\right)^3 P\int_0^{\theta_D/T}\left(\frac{x^3}{x - T_{ca}/T}\frac{1}{e^x - 1} - \frac{x^3}{x + T_{ca}/T}\frac{e^x}{e^x - 1}\right)dx \tag{13b}$$

with the simple relationship $\overline{\beta} = 2\pi\beta$. It was pointed out[2] that, due to the presence of the Cauchy principal value, Eq. (13b) may lead to a blue or to a red shift. We also observe that, since the pole in the integrand of Eq. (13b) is temperature dependent, the frequency shift may change from blue to red as the temperature is varied. The second term in Eq. (13b) corresponds to the antiresonant frequency component of the phonons. Its temperature dependence is weak.

We may also have Raman processes. In the case of acoustic phonons, using the Debye approximation, the results are given by Eqs. (24) and (25) of Ref. 3.

IV. EXPERIMENTAL RESULTS AND DISCUSSION

We first discuss the results obtained using persistent spectral hole burning. For each sample, a hole was burned at 8 K,

which as we will see may be considered as low temperature here. The hole width and position were then measured at various temperatures up to 30 K. The hole width increasing, it becomes very difficult to measure it at higher temperatures. If we have monochromatic laser beams and no saturation, Sec. III A tells us that the hole width is $\delta\omega_{\text{hole}} = 2\Gamma(0) + 2\Gamma(T)$. If we assume for simplicity the laser profile to be Lorentzian with a spectral width $\delta\omega_{\text{laser}}$, then the hole width is $\delta\omega_{\text{hole}} = 2\,\delta\omega_{\text{laser}} + 2\Gamma(0) + 2\Gamma(T)$. Working at $T = 8$ K, we first varied the pumping laser intensity and the irradiation time. We observe that, when varying the laser intensity at low saturation level and at constant irradiation time, the hole width increases linearly. This tells us that, despite the fact that we have two-photon ionization, one step is rate limiting and the relevant quantity is the irradiation dose ϕ. Such measurements also tell us which irradiation doses may be considered as low enough in that they lead to a tolerable saturation broadening.

In fact, at low irradiation doses, the hole width increases linearly with ϕ and may be written quite generally as $\delta\omega_{\text{hole}} = 2\,\delta\omega_{\text{laser}} + 2\Gamma(0)(1 + \phi/\phi_S) + 2\Gamma(T)$. ϕ_S is an effective saturation dose and saturation in the reading phase has been neglected. It is then clear that, when ϕ/ϕ_S is smaller than a few percent, the saturation broadening is smaller than the experimental uncertainty and may be neglected.

Using such a low enough irradiation dose, we then measured the hole width at various temperatures. A Lorentzian fit of the hole also gives its central frequency. The results obtained for sample *B* are shown as filled circles in Fig. 3(a) for the width and in Fig. 3(b) for the position. We observe a nonmonotonous temperature dependence of the shift. The other samples show similar behaviors. For the temperature value of 8 K, Figs. 3(a) and 3(b) show two data points, one taken immediately after burning the hole, the other one taken after the whole set of measurements. The two data points coincide, indicating a reversible behavior and proving that the frequency calibration of the laser did not change.

We then studied the global (homogeneous +inhomogeneous) linear absorption line as a function of temperature in the 8–36 K range. The global line profile is Lorentzian and a fit provides the width and the line position. Assuming a monochromatic laser beam, the line width is $\Gamma_{\text{inhom}}(T) + 2\Gamma(T)$. Again assuming a Lorentzian laser profile, the measured line width is $\delta\omega_{\text{laser}} + \Gamma_{\text{inhom}}(T) + 2\Gamma(T)$. The results are shown in Fig. 4(a) for the width and in Fig. 4(b) for the position, again for sample *B*. Looking at the error bars and/or the scatter in experimental data and comparing Fig. 3(a) with Fig. 4(a) and Fig. 3(b) with Fig. 4(b), we see that the measurement of the width and of the position is more accurate when performed on the global line than when performed on the hole.

We first compare the homogeneous width as obtained using hole burning with the global width. When plotted using the same scale and translating one set of data by 1.38 cm^{-1} vertically with respect to the other, we observe, as shown in the inset of Fig. 4(a), that the two sets of data coincide within the experimental uncertainty. This indicates that the inhomogeneous width is temperature independent in the 8–30 K range. On the other hand, if we compare the frequency shift data shown in Fig. 3(b) and in Fig. 4(b), we observe that the

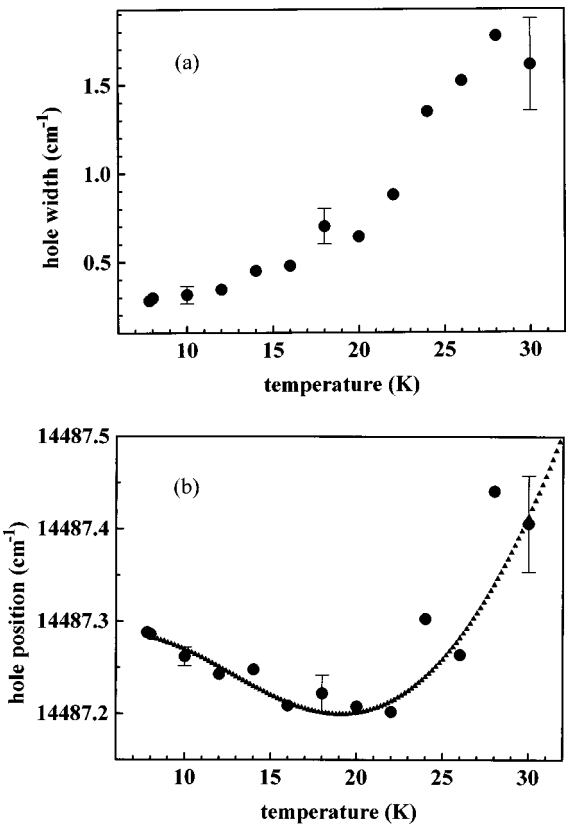

FIG. 3. Hole width (a) and hole central frequency (b) as a function of temperature. The solid circles correspond to the measurements for sample *B*. The error bars are indicated for three different temperatures. The uncertainty increases with temperature. The triangles in (b) are the theoretical predictions made using the parameters obtained when fitting the width experimental data. (See text for details.)

two sets of data cannot be made to coincide. We do not have any interpretation for this difference. We observe, however, that this difference as well as the frequency shift is on the 0.1 cm^{-1} scale and does not affect the width which is on the 1 cm^{-1} scale. The temperature dependence of Γ may then be studied using either hole burning spectroscopy or simple linear spectroscopy. The second technique does not give however the value of the low temperature $\Gamma(0)$.

To discuss the temperature dependence of the homogeneous width, we make use of the data shown in Fig. 4(a). The width increases quasiexponentially with inverse temperature. It varies very slowly at low temperature, which allows one to determine [from the data in Fig. 3(a)] the low-temperature value $\delta\omega_{\text{hole}}(0) \approx 0.26$ cm^{-1} (for sample *B*). If we take the experimental resolution into account by subtracting twice the laser spectral width from the hole width, this value agrees with the previously observed one[5] for similar concentrations. The width data cannot be fitted assuming a Raman process involving acoustic phonons (T^7 dependence at low temperature). On the contrary, as may be seen in Fig. 4(a), they are perfectly fitted if we assume a direct one-phonon absorption process. To be more precise, the global width data are fitted with the function $a_0 + \beta(e^{\hbar\omega_{ca}/k_BT} - 1)^{-1}$. The a_0 constant includes the laser spectral width, the inhomogeneous width and the low-temperature homogeneous width. (We also fitted the hole width data with the

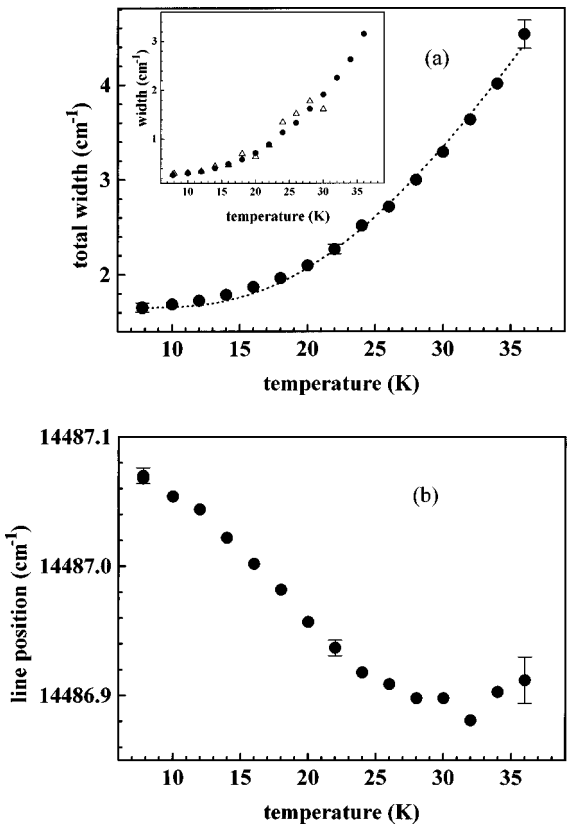

FIG. 4. Global linewidth (a) and central frequency of the global line (b) as a function of temperature. The solid circles correspond to the measurements for sample *B*, the dotted line in (a) is a fit to the experimental data assuming a one-phonon absorption process. The error bars are indicated for three different temperatures. The inset in part (a) shows how the hole width and the global linewidth may be brought to coincidence.

same function except that the constant, now denoted a_0', includes the laser spectral width and the low-temperature homogeneous width, twice each). The homogeneous width is thus comprised of a low-temperature part and of a temperature-dependent one. From the fit, it is clear that this temperature-dependent contribution mainly originates from a one-phonon absorption process, Eq. (13a), with a phonon of frequency 56 cm^{-1}, which corresponds to a temperature $T_{ca} \approx 80$ K. The low-temperature part can only be due to phonon emission processes. It turns out that these emission processes only weakly contribute to the temperature dependence of Γ. We will come back to this point below.

To discuss the temperature dependence of the frequency shift, we make use of the data shown in Fig. 3(b). The shift of the hole is more physically meaningful than the shift of the global line since, in the first case, a narrow class of sites is selected at 8 K and is then followed when the temperature is increased. From the fit of the width, we deduce the value of β and consequently of β. We may then compare the frequency shift data with the predictions of Eq. (13b) using the same value of T_{ca} and $\theta_D = 490$ K.[17] As shown in Fig. 3(b), a good agreement is obtained (this is not a fit) considering the experimental uncertainty. The model accounts for the sign of the frequency shift (assuming that level *a* is the upper level of the transition), for its nonmonotonous temperature dependence and for the temperature at which it switches from red to blue shift. At low temperature, the presence of the $p_0(\omega)$ factor heavily weighs the low-frequency modes. This explains the success of the Debye approximation and tells us at the same time that our 56 cm^{-1} phonons are acoustic phonons.

TABLE II. The parameters (in cm^{-1}) of the fit to the width data for our four samples. These parameters are defined in the text.

Sample	*A*	*B*	*C*	*D*
a_0	7.9	1.7	13.3	6.2
a_0'	0.56	0.26	0.74	0.44
β	10	10.5	11	9
ω_{ca}	43	56	44	38

In the discussion above, we concentrated on the results obtained for sample *B*. The general trends are similar for the other samples. We consistently observe, for example, a nonmonotonous temperature dependence of the frequency shift. The parameters of the fit to the width data are given in Table II. Within the uncertainty, the temperature-dependent term is sample independent. For all four samples, both data sets, homogeneous width and frequency shift, therefore indicate that a one-phonon absorption process, with a phonon frequency of 45 cm^{-1} on the average, is mainly responsible for homogeneous broadening of our 690 nm line. This is at variance with a previous report[4] concluding that the homogeneous width is well fitted when assuming a Raman process. This previous study was performed using a polarization sensitive technique. Here, using PSHB, the quantity under study is directly the homogeneous width 2Γ.

The 690 nm line corresponds to the transition between the ground state A_{1g} and the excited state T_{1u} of the Sm^{2+} ion in a cubic site (see Fig. 1). As already pointed out, the sign of the frequency shift indicates that our *a* level in Sec. III B is the upper level, T_{1u}, of our transition. This agrees with the fact that the first excited state of the Sm^{2+} ion is $\sim$256 cm^{-1} above the ground A_{1g} state. This ground state cannot then absorb a 45 cm^{-1} phonon. Referring to the notations of Sec. III B, *a* is the T_{1u} level, *b* is the A_{1g} one. The present work thus tells us that there is an eigenstate *c* of Sm^{2+} approximately 45 cm^{-1} above T_{1u}. There is no clear evidence about what this level may be. The $^7K_4$ term is split by the crystal field into 4 levels: T_{1u},A_{1u} lying 116 cm^{-1} below, E_u lying 35 cm^{-1} above A_{1u}, (Refs. 18,19) and T_{2u} located above T_{1u}. Two-photon absorption spectroscopy showed[20] that the $^5D_0$ state lies $\sim$105 cm^{-1} above T_{1u}. Our *c* level should not therefore be the $^5D_0$ one. We suggest that our *c* level, about 45 cm^{-1} above T_{1u} is the T_{2u} level.

The low-temperature width $2\Gamma(0)$ is due to one-phonon spontaneous emission from T_{1u} to $A_{1u}$and/or E_u. The transition frequencies being large (116 and 81 cm^{-1}), this explains why these phonon emission processes only weakly contribute to the temperature-dependent part of the width 2Γ. The low-temperature width $2\Gamma(0)$ is $\sim$0.1 cm^{-1}. At 30 K, the contribution of the one-phonon absorption process is $\sim$1.4 cm^{-1}. Since the phonon occupation number p_0 is then about 0.13, this means that the $T_{2u} \leftarrow T_{1u}$ transition is about 100 times more probable than the $T_{1u} \rightarrow A_{1u}, E_u$ ones. This may be understood as follows. The acoustic phonons in CaF_2 may be divided into deformational A_{1g}, E_g, and T_{2g} phonons

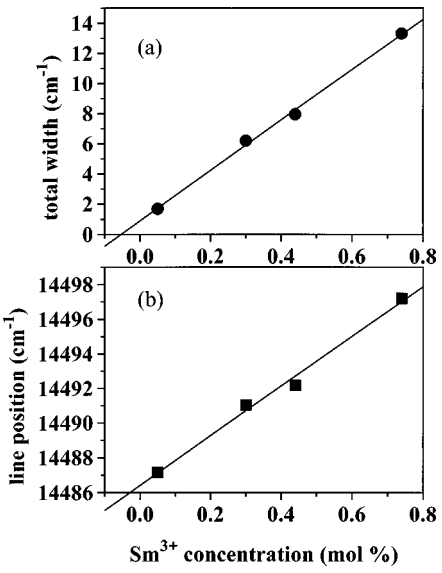

FIG. 5. Width (a) and position (b) of the inhomogeneous distribution as a function of the Sm^{3+} concentration for samples $A-D$. The solid circles and squares are the experimental data, the solid lines are linear fits.

and rotational T_{1g} phonons, the latter originating from TA modes only.[18] Since $T_{1u}\times A_{1u}=T_{1g}$, the $T_{1u}\rightarrow A_{1u}$ transition is only due to the rotational phonons. Since $T_{1u}\times E_u=T_{1g}+T_{2g}$, the $T_{1u}\rightarrow E_u$ transition is in principle due to both rotational T_{1g} and deformational T_{2g} phonons. But, according to Akimov and Kaplyanskii,[18] the matrix element of the C operator, Eq. (5), vanishes for T_{2g} phonons so that the $T_{1u}\rightarrow E_u$ transition is also only due to rotational phonons and is in fact less probable than the $T_{1u}\rightarrow A_{1u}$ one. Finally, since $T_{1u}\times T_{2u}=A_{2g}+E_g+T_{1g}+T_{2g}$, the $T_{2u}\leftarrow T_{1u}$ transition is due to both rotational T_{1g} and deformational E_g phonons. It turns out[18] that the E_g phonons are very effective since the $E_u\rightarrow A_{1u}$ transition ($A_{1u}\times E_u=E_g$) is 100 times more probable than the $T_{1u}\rightarrow A_{1u}$ one. Furthermore, the direct transition rates are proportional to the cube of the transition frequency. This adds a further factor of 2 when going from 35 ($E_u\rightarrow A_{1u}$) to 45 ($T_{2u}\leftarrow T_{1u}$) cm^{-1}. It thus seems reasonable to have a dominant one-phonon absorption process.

As already mentioned, the general trends are similar for the other samples. We observe however that the inhomogeneous width is sample dependent. Our samples contain a fairly large concentration of Sm^{3+}-F^- complexes which act as point defects. Due to γ irradiation, we also have self-trapped hole pairs for samples C and D, but their concentration is about 100 times smaller. It has been shown theoretically[12] that inhomogeneous broadening due to point defects by random strains and field gradients leads to a Lorentzian distribution, the width and frequency shift being proportional to the concentration of point defects. Plotting the inhomogeneous width and the low-temperature line frequency of samples A–D as a function of Sm^{3+} concentration in Fig. 5, we observe such a linear correlation. The residual inhomogeneous width at zero Sm^{3+} concentration that is visible in Fig. 5(a) is probably due to other mechanisms: dislocations, other point defects . . . .

Experiment also shows that the low-temperature homogeneous width is sample dependent. In the case of mixed CaF_2/YF_3 and CaF_2/LaF_3 matrices doped with Eu^{3+} or Pr^{3+}, it has been observed that the homogeneous width depends on the Y or La concentrations.[21] In these disordered matrices, a contribution of tunneling two-level systems has been suggested to explain the linear temperature dependence of the hole width. Our samples contain Sm^{3+} ions and are therefore mixed CaF_2/SmF_3 crystals but with a low Sm content. The 690 nm transition being interconfigurational ($4f$-$5d$) is however more sensitive to the crystal field than the ($4f$-$4f$) transitions of Eu^{3+} and Pr^{3+}. This could explain the sample dependence of the homogeneous width which we observe to increase with Sm^{3+} concentration. We note, however, that the dominant dephasing mechanism is always one-phonon absorption in our case.

V. CONCLUSION

Using persistent spectral hole burning spectroscopy, we studied the homogeneous broadening of the 690 nm line in the CaF_2:Sm^{2+} model system. We burned a hole at low temperature (8 K) and measured its width and central frequency as a function of temperature up to 30 K. We show, in the theory part, how this may lead to the determination of the temperature-dependent homogeneous width. We observe a nonmonotonous frequency shift in such a system. The data show that the inhomogeneous width is temperature independent. Fitting the data for the temperature-dependent hole width, we conclude that homogeneous broadening is mainly due to a one-phonon absorption process, the (acoustic) phonon frequency being $\sim$45 cm^{-1}. This conclusion is supported by the fact that the theoretical prediction of the shift obtained using the parameters deduced from the fit to the width data is in perfect agreement with the experiment. These measurements and their interpretation also tell us that the Sm^{2+} ion possesses a level $\sim$45 cm^{-1} above the T_{1u} level that we suggest to be the T_{2u} level. The inhomogeneous distribution is Lorentzian and its width and position depend on the Sm^{3+} concentration (the Sm^{3+}-F^- complexes acting as point defects) exactly as predicted by theory.

This work as well as Ref. 3 demonstrate how the simultaneous measurement of both the width and frequency shift renders the understanding of the broadening mechanism more unambiguous. This is a great advantage of PSHB spectroscopy.

ACKNOWLEDGMENTS

The authors would like to thank F. Auzel, T. T. Basiev, V. V. Fedorov, and A. Ya. Karazik for loan of the samples.

[1] W. E. Moerner, *Persistent Spectral Hole Burning: Science and Applications* (Springer-Verlag, Berlin, 1988).
[2] See, for example, W. M. Yen, W. C. Scott, and A. L. Shawlow, Phys. Rev. **136**, A271 (1964).
[3] W. Beck, D. Ricard, and C. Flytzanis, Phys. Rev. B **57**, 7694 (1998).
[4] J. H. Lee, J. J. Song, M. A. F. Scarparo, and M. D. Levenson, Opt. Lett. **5**, 196 (1980).
[5] R. M. Macfarlane and R. M. Shelby, Opt. Lett. **9**, 533 (1984).
[6] W. Beck, V. V. Fedorov, D. Ricard, C. Flytzanis, and T. T. Basiev (unpublished).
[7] W. Kaiser, C. G. B. Garrett, and D. L. Wood, Phys. Rev. **123**, 766 (1961).
[8] W. Beck, D. Ricard, and C. Flytzanis, Appl. Phys. Lett. **69**, 3197 (1996).
[9] A. Winnacker, R. M. Shelby, and R. M. Macfarlane, Opt. Lett. **10**, 350 (1985).
[10] A. Renn, A. J. Meixner, U. P. Wild, and F. A. Burkhalter, Chem. Phys. **93**, 157 (1985).
[11] A. J. Meixner, A. Renn, and U. P. Wild, J. Chem. Phys. **91**, 6728 (1989).
[12] A. M. Stoneham, Rev. Mod. Phys. **41**, 82 (1969).
[13] H. de Vries and D. A. Wiersma, J. Chem. Phys. **72**, 1851 (1980).
[14] D. Haarer, in *Persistent Spectral Hole Burning: Science and Applications* (Ref. 1), p. 79.
[15] N. Peyghambarian, B. Fluegel, D. Hulin, A. Migus, M. Joffre, A. Antonetti, S. W. Koch, and M. Lindberg, IEEE J. Quantum Electron. **25**, 2516 (1989).
[16] R. Jaaniso and H. Bill, Europhys. Lett. **16**, 569 (1991).
[17] M. M. Elcombe and A. W. Pryor, J. Phys. C **3**, 492 (1970).
[18] A. V. Akimov and A. A. Kaplyanskii, Fiz. Tverd. Tela **23**, 3326 (1981) [Sov. Phys. Solid State **23**, 1932 (1981)].
[19] R. M. Macfarlane, W. S. Brocklesby, P. D. Bloch, and R. T. Harley, Opt. Commun. **58**, 25 (1986).
[20] R. L. Fuller and D. S. McClure, J. Lumin. **45**, 354 (1990).
[21] K. W. Jang, K. S. Hong, T. T. Basiev, and R. S. Meltzer, J. Lumin. **66&67**, 8 (1996).